RESEARCH ARTICLE

Check for updates

Bioorthogonal activation and mitochondrial targeting of a near-infrared-emitting iridium(III) nitrone complex via cyclooctynylated phosphonium cations for enhanced cellular imaging and photodynamic therapy†

Edward R. H. Walter, [ID] ‡[a,b] Lawrence Cho-Cheung Lee, [ID] ‡[b,c] Peter Kam-Keung Leung, [ID] ‡[c,d] Kenneth Kam-Wing Lo [ID] *[c,d] and Nicholas J. Long [ID] *[a]

In this work, we designed and synthesised a new cyclometallated iridium(III) nitrone complex [Ir(bpz)$_2$(bpy-nitrone)](PF$_6$) (**1**) (Hbpz = benzo[a]phenazine; bpy-nitrone = 4-((methyl(oxido)imino)methyl)-4′-methyl-2,2′-bipyridine) as a bioorthogonally activatable phototheranostic agent. Complex **1** displayed very weak emission and singlet oxygen ($^1O_2$) photosensitisation in solutions due to the quenching nitrone moiety. However, upon the strain-promoted alkyne−nitrone cycloaddition (SPANC) reaction with bicyclo[6.1.0]non-4-yne (BCN), which converted the nitrone unit to a non-quenching isoxazoline derivative, the complex exhibited a substantial increase in emission intensity in the near-infrared region and $^1O_2$ generation efficiency. Given that mitochondria are a crucial target in cancer therapy, we prepared a series of BCN-functionalised phosphonium cations (**BCN-Phos-n**), each bearing different substituents, to serve as mitochondrial-targeting vectors for delivering complex **1** to the mitochondria via the bioorthogonal SPANC reaction. Notably, complex **1** exhibited more significant emission turn-on upon reaction with **BCN-Phos-5** and **BCN-Phos-6** (I/I_o = 24.7 and 14.1, respectively), attributed to their increased hydrophobicity resulting from the methylation or methoxylation of the phenyl rings on the phosphonium cation. Live-cell confocal imaging and flow cytometric analyses revealed that complex **1** showed larger emission enhancement in HeLa cells pretreated with **BCN-Phos-5** or **BCN-Phos-6** compared to other **BCN-Phos-n** analogues. Co-staining experiments confirmed that the resultant luminescent isoxazoline cycloadducts predominantly accumulated in the mitochondria. Additionally, both dark and light-induced cytotoxicity of complex **1** increased upon pretreatment of the cells with **BCN-Phos-5** or **BCN-Phos-6**. Our results demonstrate that the theranostic potential of transition metal nitrone complexes can be significantly enhanced via strategic structural manipulation of their bioorthogonal reaction partners.

[a]*Department of Chemistry, Imperial College London,*
Molecular Sciences Research Hub, W12 0BZ, UK. E-mail: n.long@imperial.ac.uk
[b]*Laboratory for Synthetic Chemistry and Chemical Biology Limited, Units 1503-1511,*
15/F, Building 17 W, Hong Kong Science Park, New Territories, Hong Kong,
P. R. China
[c]*Department of Chemistry, City University of Hong Kong, Tat Chee Avenue, Kowloon,*
Hong Kong, P. R. China. E-mail: bhkenlo@cityu.edu.hk
[d]*State Key Laboratory of Terahertz and Millimetre Waves,*
City University of Hong Kong, Tat Chee Avenue, Kowloon, Hong Kong, P. R. China
†Electronic supplementary information (ESI) available. See DOI: https://doi.org/10.1039/d5qi01139f
‡ Equal contribution from these authors.

Introduction

Over the past two decades, the development of bioorthogonal chemistry[1,2] has revolutionised the fields of chemical biology[3–5] and biomedicine.[6–8] Bioorthogonal ligation reactions between two abiotic functionalities have enabled the visualisation of specific biomolecules and associated biological events in live cells using fluorescence microscopy.[9] The use of fluorescent probes, however, can lead to unavoidable background fluorescence due to non-specific covalent labelling and the entrapment of unreacted probes within the cellular environment. Thus, there has been significant interest in the development of fluorogenic bioorthogonal probes, whose fluorescence is quenched by the appended bioorthogonal group

and can only be restored upon specific bioorthogonal reactions, thereby enhancing the precision of fluorescence imaging.[10–12] This design strategy has recently been extended to the development of activatable photosensitisers for targeted photodynamic therapy (PDT).[13,14] The controlled activation of the reactive oxygen species (ROS) photosensitisation capabilities of the photosensitisers through bioorthogonal reactions can minimise undesirable off-target photodamage often observed with traditional photosensitisers, which display "always-on" photosensitisation properties and lack target selectivity.

Luminescent and photofunctional transition metal complexes have gained significant attention as phototheranostics due to their attractive photophysical and photochemical properties, including high photostability, long-lived and environment-sensitive emission, as well as efficient ROS photosensitisation.[15–19] We have a long-standing interest in the development of these complexes as bioorthogonal reagents for various biological and biomedical applications.[20] In 2016, we demonstrated for the first time that nitrone, a 1,3-dipole that can selectively react with cyclooctynes *via* the strain-promoted alkyne–nitrone cycloaddition (SPANC) reaction,[21] can serve as an emission quencher for transition metal complexes, providing a new avenue for the development of phosphorogenic bioorthogonal probes.[22,23] The nitrone-modified complexes are non-emissive in solutions, but exhibit significant emission enhancement upon reaction with bicyclo[6.1.0]non-4-yne (BCN) derivatives (Scheme 1). This modification also allows for the modulation of the ROS photosensitisation efficiencies of the complexes, enabling controlled activation of their emission and ROS generation behaviour in targeted
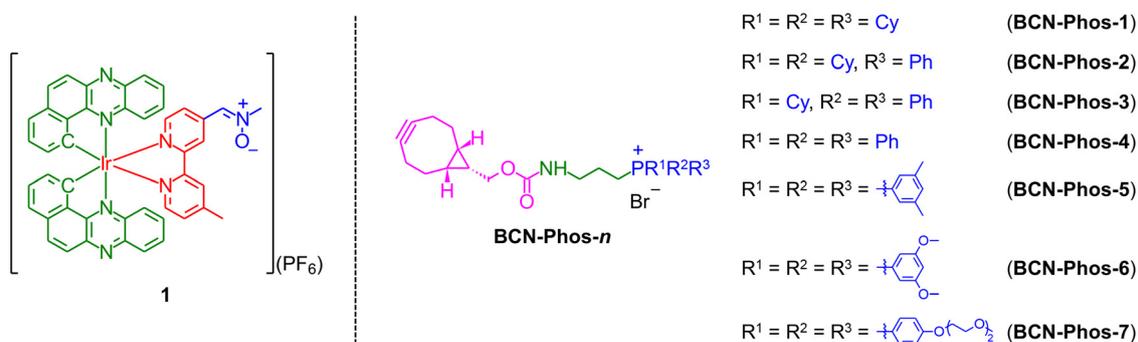
cells.[24,25] Thus, transition metal nitrone complexes represent a promising scaffold for the development of bioorthogonally activatable probes and photosensitisers.

Mitochondria are crucial subcellular organelles involved in a wide range of important biological processes including energy production,[26] biomolecular synthesis,[26] calcium signalling,[27] as well as cell proliferation and death.[28] Mitochondrial dysfunction can lead to various diseases such as cancer[29] and neurodegenerative disorders.[30] Given their pivotal role in maintaining cellular functions, mitochondria have become an important target for cancer therapy.[31] Mitochondria possess a negative membrane potential (*ca.* −120 to −180 mV), and it has been reported that the mitochondria in cancer cells are more hyperpolarised than in normal cells due to their higher metabolic activity.[32] Thus, lipophilic cations such as triphenylphosphonium cation (TPP$^+$) preferentially accumulate in the mitochondria over other subcellular organelles, resulting in *ca.* 100–1000-fold higher intramitochondrial concentrations.[33] These moieties have been engineered with various bioorthogonal handles to precisely direct fluorescent/fluorogenic bioorthogonal probes to the mitochondria, facilitating the imaging of these organelles in live cells.[34–46] This approach enables the monitoring of mitochondrial membrane potential changes[47] and mitophagy,[48] as well as the activation of mitochondria-enriched prodrugs for applications in cancer therapy[49–53] and cardioprotection.[54] However, the use of a two-step bioorthogonal approach for delivering photoactive transition metal complexes to the mitochondria, and controlled activation of their emission and ROS photosensitisation properties for bioimaging and PDT applications remains unexplored.

In this work, we designed, synthesised and characterised a new cyclometallated iridium(III) nitrone complex [Ir(bpz)$_2$(bpy-nitrone)](PF$_6$) (**1**) (Hbpz = benzo[*a*]phenazine; bpy-nitrone = 4-((methyl(oxido)imino)methyl)-4′-methyl-2,2′-bipyridine) (Scheme 2) as a bioorthogonally activatable phototheranostic agent. The Hbpz ligand was selected because its metal complexes show near-infrared (NIR) emission and high singlet oxygen ($^1O_2$) generation efficiencies.[55] Additionally, we prepared a series of BCN-modified phosphonium cations (**BCN-Phos-*n***) (Scheme 2) as mitochondrial-targeting vectors to

Scheme 1 The SPANC reaction of phosphorogenic iridium(III) nitrone complexes with BCN derivatives leading to the formation of luminescent isoxazoline cycloadducts.

R^1 = R^2 = R^3 = Cy	(**BCN-Phos-1**)
R^1 = R^2 = Cy, R^3 = Ph	(**BCN-Phos-2**)
R^1 = Cy, R^2 = R^3 = Ph	(**BCN-Phos-3**)
R^1 = R^2 = R^3 = Ph	(**BCN-Phos-4**)
R^1 = R^2 = R^3 =	(**BCN-Phos-5**)
R^1 = R^2 = R^3 =	(**BCN-Phos-6**)
R^1 = R^2 = R^3 =	(**BCN-Phos-7**)

Scheme 2 Structures of complex **1** and **BCN-Phos-*n***.

This journal is © the Partner Organisations 2025

Inorg. Chem. Front., 2025, **12**, 6484–6493 | **6485**

direct the nitrone complex to the mitochondria *via* the SPANC reaction. Specifically, **BCN-Phos-1–BCN-Phos-4** carried varying numbers of cyclohexyl (Cy) and phenyl (Ph) moieties on the phosphonium cation to tune their aromaticity;[56–58] while **BCN-Phos-5–BCN-Phos-7** contained different substituents on the phenyl rings of the TPP$^+$ unit, including two methyl (**BCN-Phos-5**) or methoxy groups (**BCN-Phos-6**) at the *meta*-positions to enhance their lipophilicity,[59–62] or a di(ethylene glycol) pendant at the *para*-position (**BCN-Phos-7**) to increase its aqueous solubility and biocompatibility.[57,58]

Results and discussion

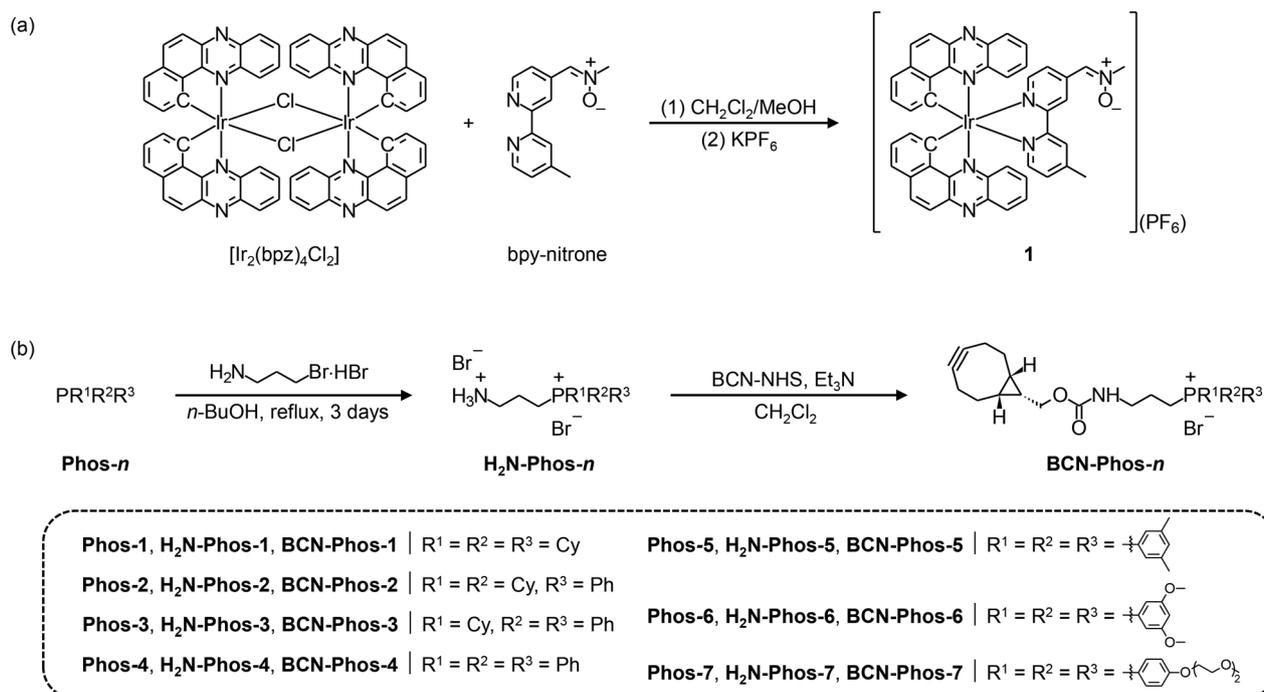### Synthesis and characterisation of complex 1 and BCN-Phos-*n*

The synthesis of complex **1** involved the reaction of the dichloro-bridged iridium(III) dimer [Ir$_2$(bpz)$_4$Cl$_2$] with the ligand bpy-nitrone in CH$_2$Cl$_2$/MeOH (Scheme 3a), followed by anion exchange with KPF$_6$ and purification by column chromatography and recrystallisation from CH$_2$Cl$_2$/Et$_2$O. The complex was characterised by high resolution (HR)-ESI-MS, ^{1}H and ^{13}C NMR and IR spectroscopy, and gave satisfactory elemental analyses (ESI†).

The BCN-modified phosphonium cations **BCN-Phos-*n*** were synthesised using the corresponding phosphine precursors (**Phos-*n***) (Scheme 3b), which were either purchased from commercial suppliers (for **Phos-1–Phos-4**) or prepared according to previously reported protocols (for **Phos-5–Phos-7**).[63,64] The phosphine precursors were reacted with 3-bromopropylamine hydrobromide in *n*-butanol under reflux for 3 days, in a pro-

cedure adapted from Zhou and co-workers.[65] The resultant amine-functionalised phosphines (**H$_2$N-Phos-*n***) were obtained as ammonium salts in good yields (44–62%) after purification by recrystallisation from isopropanol/Et$_2$O, except for **H$_2$N-Phos-1** which did not precipitate out of Et$_2$O and was, therefore, used in subsequent steps without further purification. Amide coupling of **H$_2$N-Phos-*n*** with (1*R*,8*S*,9*S*)-bicyclo [6.1.0]non-4-yn-9-ylmethyl *N*-succinimidyl carbonate (BCN–NHS) was achieved under mild basic conditions.[22–25] All **BCN-Phos-*n*** analogues were obtained in average to good yields (45–78%) after purification by silica gel column chromatography. These compounds were characterised by HR-ESI-MS and ^{1}H, ^{13}C and ^{31}P NMR spectroscopy (ESI†).

Photophysical and photochemical properties of complex 1

Complex **1** displayed intense spin-allowed intraligand (^{1}IL) ($\pi \rightarrow \pi^*$) (bpy-nitrone and bpz) absorption in the UV region (*ca.* 274–431 nm, ε on the order of 10^4 dm^3 mol^{-1} cm^{-1}) and weaker spin-allowed metal-to-ligand charge-transfer (^{1}MLCT) (dπ(Ir) $\rightarrow \pi^*$(bpy-nitrone and bpz)) absorption features in the visible region (*ca.* 456–550 nm) (Fig. 1a and Table S1, ESI†).[25,55] The strong absorption in the region of 500–600 nm is an attractive feature because it allows for efficient photo-excitation using green light. The weaker absorption tailing beyond *ca.* 615 nm is assigned to spin-forbidden ^{3}MLCT (dπ(Ir) $\rightarrow \pi^*$(bpy-nitrone and bpz)) transitions. Upon photoirradiation, the complex exhibited NIR emission in fluid solutions at 298 K (Table 1 and Fig. 1b). Additionally, it showed a vibronically structured emission band with an extraordinarily long emission lifetime (8.79 μs) in an alcohol glass at 77 K (Table 1

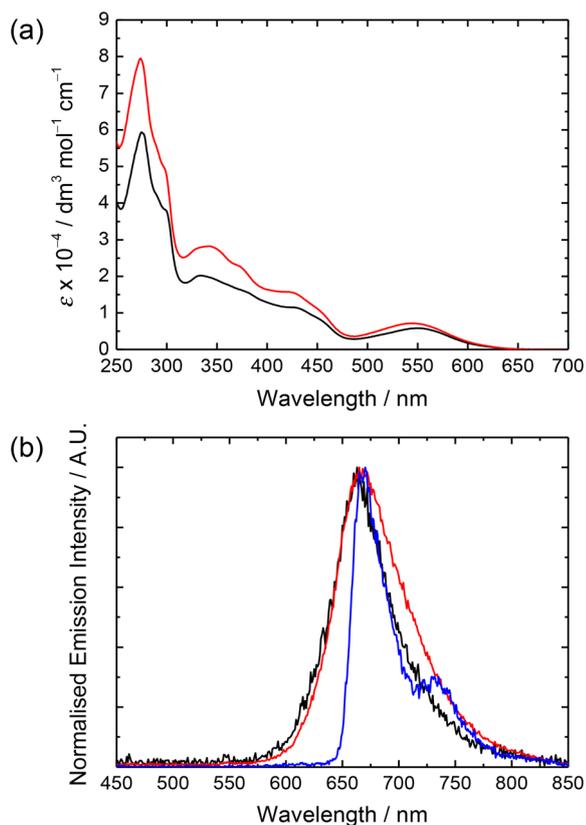**Scheme 3** Synthetic routes of (a) complex **1** and (b) BCN-Phos-*n*.

6486 | *Inorg. Chem. Front.*, 2025, **12**, 6484–6493

This journal is © the Partner Organisations 2025

Fig. 1 (a) Electronic absorption and (b) normalised emission spectra of complex **1** in CH$_2$Cl$_2$ (black) and CH$_3$CN (red) at 298 K and in alcohol glass at 77 K (blue).

Table 1 Photophysical data and ^{1}O$_2$ generation quantum yields (Φ_Δ) of complexes **1** and **1-BCN**

Complex	Medium (T/K)	$\lambda_{em}{}^a$/nm	$\tau_o{}^b$/μs	$\Phi_{em}{}^c$	$\Phi_\Delta{}^d$
1	CH$_2$Cl$_2$ (298)	664	4.80	0.0047	
	CH$_3$CN (298)	668	2.97	0.0043	0.05
	Glass^e (77)	668, 730 sh	8.79		
1-BCN	CH$_2$Cl$_2$ (298)	666	4.28	0.072	
	CH$_3$CN (298)	668	2.67	0.062	0.76
	Glass^e (77)	667, 729 sh	9.63		

^{a} λ_{ex} = 350 nm. ^{b} The lifetimes were measured at the emission maxima (λ_{ex} = 355 nm). ^{c} The Φ_{em} values were determined in degassed solvents using [Ru(bpy)$_3$]Cl$_2$ (Φ_{em} = 0.040 in aerated H$_2$O, λ_{ex} = 455 nm)[66] as a reference. ^{d} The Φ_Δ values were determined in aerated solvents using [Ru(bpy)$_3$]Cl$_2$ (Φ_Δ = 0.57 in aerated CH$_3$CN, λ_{ex} = 450 nm)[67] as a reference. ^{e} EtOH/MeOH (4 : 1, v/v).

and Fig. 1b). These observations suggest that the emission of the complex originates from a predominant ^{3}IL ($\pi \rightarrow \pi^*$) (bpz) excited state with possible mixing of some ^{3}MLCT (dπ(Ir) $\rightarrow \pi^*$ (bpy-nitrone/bpz)) character.[25,55] Similar emission features were observed when the complex was excited at 550 nm, indicating that the emission is largely independent of the excitation wavelength. Importantly, the emission quantum yields of the complex ($\Phi_{em} \leq 0.0047$; Table 1) were significantly lower

than those of related bpz complexes,[55] indicating efficient emission quenching by the appended nitrone unit.[22–25] Additionally, the ^{1}O$_2$ generation quantum yield (Φ_Δ) of the complex was determined by monitoring the emission band of ^{1}O$_2$ centred at *ca.* 1270 nm in aerated CH$_3$CN. The small Φ_Δ value (0.05; Table 1) indicates strong suppression of the ^{1}O$_2$ photosensitisation capability of the complex by the quenching nitrone moiety.

Bioorthogonal reactivity and phosphorogenic response of complex 1

We utilised the strained alkyne (1*R*,8*S*,9*S*)-bicyclo[6.1.0]non-4-yn-9-ylmethanol (BCN–OH) as a model substrate to examine the bioorthogonal reactivity of the nitrone complex. The second-order rate constant (k_2) of the SPANC reaction of the complex with BCN–OH in MeOH at 298 K was determined to be 0.3309 M^{-1} s^{-1} (Fig. S1, ESI†), which is 8.3 times greater than that of the free ligand bpy-nitrone (k_2 = 0.040 M^{-1} s^{-1}).[22] The accelerated reaction kinetics can be attributed to the direct coordination of the nitrone ligand to the cationic iridium(III) polypyridine unit, which enhanced its reactivity.[22–25] Importantly, upon the SPANC reaction with BCN–OH in aerated phosphate-buffered saline (PBS; pH 7.4)/ MeOH (9 : 1, v/v), the complex showed substantial emission enhancement (I/I_o = 5.8; Table 2 and Fig. 2a) and lifetime extension (τ increased from 0.05 to 0.13 μs; Table 2), resulting from the conversion of the quenching nitrone moiety to a non-quenching isoxazoline derivative. The formation of the isoxazoline product **1-BCN** was verified by ESI-MS analysis (Fig. S2, ESI†). Conjugate **1-BCN** was isolated and purified, and its photophysical and ^{1}O$_2$-photogeneration properties were investigated. Both Φ_{em} (0.062–0.072; Table 1) and Φ_Δ (0.76; Table 1) values of conjugate **1-BCN** are larger than those of complex **1** ($\Phi_{em} \leq 0.0047$, Φ_Δ = 0.05; Table 1). These results confirm that both the emission and ^{1}O$_2$-photosensitisation properties of complex **1** can be activated through the bioorthogonal SPNAC reaction with BCN derivatives, which effectively eliminates the nitrone-associated quenching pathway.

Table 2 Emission wavelengths (λ_{em}), emission enhancement factors (I/I_o) and emission lifetimes (τ) of complex **1** (10 μM) upon reaction with BCN–OH or **BCN-Phos-n** (250 μM) in aerated PBS (pH 7.4)/MeOH (9 : 1, v/v) at 298 K for 24 h

Entry	λ_{em}	$I/I_o{}^a$	τ/μs
1	695	—	0.05
1 + BCN–OH	684	5.8	0.13
1 + **BCN-Phos-1**	687	4.2	0.15
1 + **BCN-Phos-2**	690	3.8	0.14
1 + **BCN-Phos-3**	703	3.1	0.12
1 + **BCN-Phos-4**	686	3.3	0.13
1 + **BCN-Phos-5**	674	24.7	0.33
1 + **BCN-Phos-6**	677	14.1	0.25
1 + **BCN-Phos-7**	706	4.5	0.19

^{a} I_o and I are the emission intensities of the complex (10 μM) in the absence and presence of BCN–OH or **BCN-Phos-n** (250 μM), respectively.

This journal is © the Partner Organisations 2025

Inorg. Chem. Front., 2025, **12**, 6484–6493 | **6487**
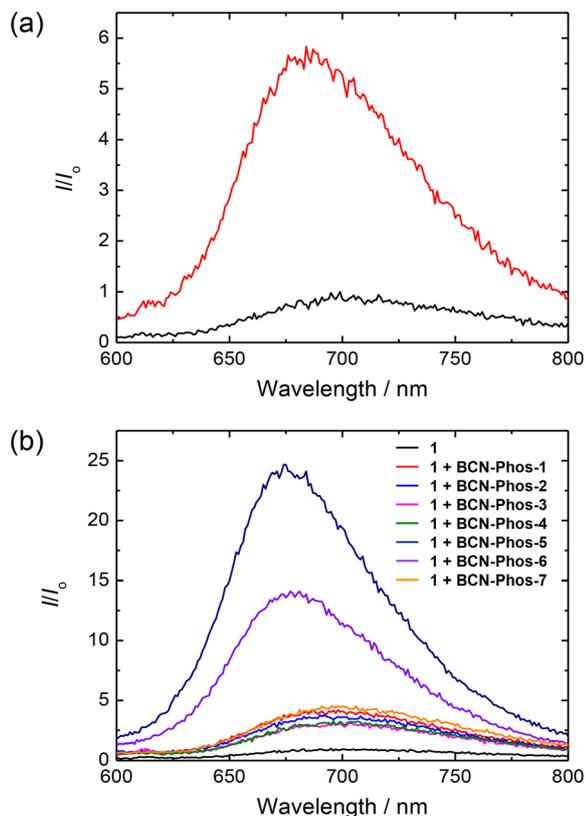
Fig. 2 (a) Emission spectra of complex **1** (10 μM) in the absence (black) and presence of BCN−OH (250 μM) (red) in aerated PBS (pH 7.4)/MeOH (9 : 1, v/v) upon incubation at 298 K for 24 h. (b) Emission spectra of complex **1** (10 μM) in the absence (black) and presence of **BCN-Phos-1** (red), **BCN-Phos-2** (blue), **BCN-Phos-3** (magenta), **BCN-Phos-4** (olive), **BCN-Phos-5** (navy), **BCN-Phos-6** (violet) and **BCN-Phos-7** (orange) (250 μM) in aerated PBS (pH 7.4)/MeOH (9 : 1, v/v) upon incubation at 298 K for 24 h. Excitation wavelength = 350 nm.

We also investigated the phosphorogenic response of complex **1** towards the **BCN-Phos-*n*** derivatives. Incubation of complex **1** with the **BCN-Phos-*n*** analogues in aerated aqueous buffers led to substantial emission enhancement (I/I_o = 3.1–24.7) and lifetime extension (τ = 0.12–0.33 μs) (Table 2 and Fig. 2b). Notably, the **BCN-Phos-5** and **BCN-Phos-6** treatment resulted in a larger increase in emission intensity (I/I_o = 24.7 and 14.1) and lifetime (τ = 0.33 and 0.25 μs), accompanied by a notable blue shift in the emission maximum from 695 nm to 674 and 677 nm, respectively (Table 2 and Fig. 2b). The more significant photophysical changes compared to other **BCN-Phos-*n*** analogues are likely due to the formation of a more hydrophobic pendant after reaction with **BCN-Phos-5** and **BCN-Phos-6**, which feature two lipophilic methyl or methoxy groups on each of the phenyl rings of the TPP$^+$ unit, resulting in a greater reduction in the polarity of the proximal environment of the complex. Such a result aligns with our previous observations that luminescent iridium(III) polypyridine complexes display higher emission intensities and longer lifetimes in less polar solvents or upon bioconjugation to proteins.[68–73]

Cellular uptake, localisation and (photo)cytotoxicity of complex 1

We then studied the phosphorogenic response of the nitrone complex towards the **BCN-Phos-*n*** derivatives in live HeLa cells. The cells were first incubated with **BCN-Phos-*n*** (5 μM) for 2 h, washed with PBS (pH 7.4), and then treated with complex **1** (5 μM) for an additional 2 h prior to imaging. Laser-scanning confocal microscopy (LSCM) images reveal negligible emission from HeLa cells incubated with complex **1** (Fig. 3a). However, intense intracellular emission was observed upon pretreatment
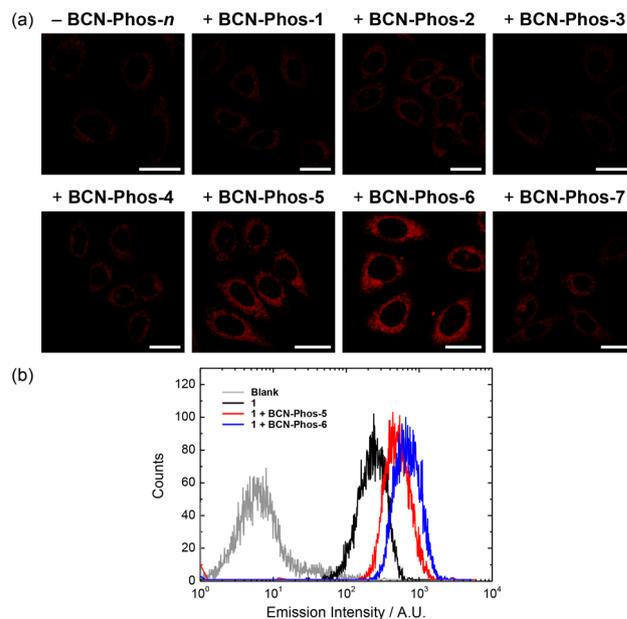

Fig. 3 (a) LSCM images of HeLa cells incubated with complex **1** (5 μM, 2 h; λ_{ex} = 488 nm, λ_{em} = 650–750 nm) without or with pretreatment of **BCN-Phos-*n*** (5 μM, 2 h) at 37 °C. Scale bar = 25 μm. (b) Flow cytometric results of HeLa cells under different treatment. The cells were treated with blank medium (2 h) (grey); complex **1** (5 μM, 2 h) (black); **BCN-Phos-5** (5 μM, 2 h) and then complex **1** (5 μM, 2 h) (red); and **BCN-Phos-6** (5 μM, 2 h) and then complex **1** (5 μM, 2 h) (blue) at 37 °C.
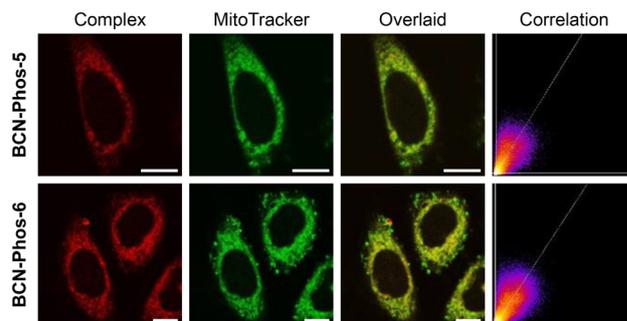

Fig. 4 LSCM images of HeLa cells pretreated with **BCN-Phos-5** or **BCN-Phos-6** (5 μM, 2 h) and then incubated with complex **1** (5 μM, 2 h; λ_{ex} = 488 nm, λ_{em} = 650–750 nm) and MitoTracker Green (100 nM, 30 min; λ_{ex} = 488 nm, λ_{em} = 506–526 nm) at 37 °C. Scale bar = 10 μm. PCC = 0.79 (**BCN-Phos-5**) and 0.81 (**BCN-Phos-6**).
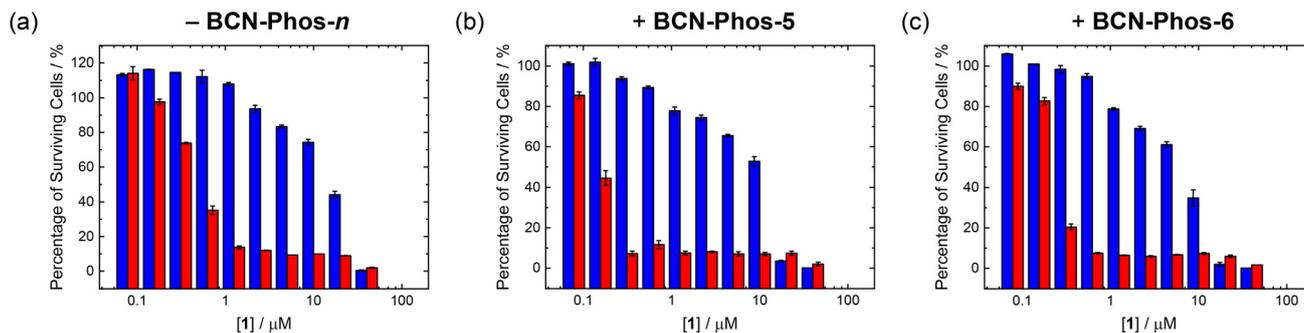
Fig. 5 Viability of HeLa cells incubated with (a) blank medium, (b) **BCN-Phos-5** (5 μM) or (c) **BCN-Phos-6** (5 μM) for 2 h and then treated with complex **1** at different concentrations for 2 h, followed by incubation in the dark (blue) or irradiation at 525 nm (10 mW cm^{-2}) (red) for 5 min, and then further incubated with blank medium for 20 h.

of the cells with **BCN-Phos-5** or **BCN-Phos-6** (Fig. 3a). Flow cytometric analysis confirmed that complex **1**-treated cells exhibited a 2.15- and 2.94-fold increase in emission intensity when pretreated with **BCN-Phos-5** and **BCN-Phos-6**, respectively (Fig. 3b and Table S2, ESI†). Additionally, ICP-MS analysis indicated that the cellular uptake of complex **1** remained similar without (1.83 fmol per cell) and with pretreatment of **BCN-Phos-5** and **BCN-Phos-6** (1.77 and 1.74 fmol per cell, respectively) (Table S3, ESI†). These results confirm that the observed intracellular emission enhancement is attributable to the SPANC reaction of complex **1** with **BCN-Phos-5** and **BCN-Phos-6**, rather than an increase in cellular accumulation of the complex. However, similar emission enhancement was not observed for cells pretreated with other **BCN-Phos-n** derivatives (Fig. 3a and S3 and Table S2, ESI†), consistent with their smaller emission enhancement in solutions (I/I_0 = 3.1–4.5; Table 2 and Fig. 2b). Co-staining experiments with MitoTracker Green showed that the luminescent isoxazoline cycloadducts formed from the reaction of complex **1** with **BCN-Phos-5** and **BCN-Phos-6** were enriched in the mitochondrial region of the cells, with Pearson's correlation coefficients (PCC's) of 0.79 and 0.81, respectively (Fig. 4). The mitochondrial accumulation of the isoxazoline cycloadducts is likely due to their cationic and lipophilic character.[74–80]

We also examined the (photo)cytotoxicity of complex **1** towards HeLa cells with or without **BCN-Phos-n** pretreatment using the Neutral Red uptake (NRU) assay. Complex **1** exhibited moderate dark cytotoxicity (IC$_{50,\text{dark}}$ = 18 μM) and substantially enhanced photocytotoxic activity (IC$_{50,\text{light}}$ = 0.37 μM) upon irradiation at 525 nm (10 mW cm^{-2}) for 5 min (Fig. 5a and Table S4, ESI†). Notably, the (photo)cytotoxicity of the complex was further increased when the cells were pretreated with **BCN-Phos-5** or **BCN-Phos-6,** with IC$_{50,\text{dark}}$ values decreasing to 9.6 and 6.3 μM and IC$_{50,\text{light}}$ values decreasing to 0.14 and 0.22 μM, respectively (Fig. 5b and c and Table S4, ESI†). The enhanced dark cytotoxicity of the complex can be attributed to its increased accumulation in the mitochondria after the SPANC reaction with **BCN-Phos-5** or **BCN-Phos-6,** which probably interferes with mitochondrial functions.[79] Notably, the photocytotoxicity of the complex was further enhanced fol-

lowing the reaction, which is attributed to the increased $^1O_2$ generation by the resultant isoxazoline cycloadducts. These results highlight that the therapeutic potential of the complex can be enhanced *via* a judicious selection of its bioorthogonal reaction partners.

Conclusions

In summary, we developed a novel iridium(III) nitrone complex as a bioorthogonally activatable phototheranostic agent, and a series of BCN-modified phosphonium cations serving as mitochondrial-targeting vectors to direct the nitrone complex to the mitochondria *via* the bioorthogonal SPANC reaction for imaging and PDT applications. Notably, the complex displayed more pronounced emission turn-on upon reaction with **BCN-Phos-5** and **BCN-Phos-6** compared to other **BCN-Phos-n** analogues, attributed to the presence of additional hydrophobic methyl or methoxy groups on the phenyl rings of the TPP$^+$ unit that resulted in a more hydrophobic pendant. Similar emission changes were observed in live cells pretreated with **BCN-Phos-5** or **BCN-Phos-6**. Owing to their cationic and lipophilic character, the resultant luminescent isoxazoline cycloadducts were enriched in the mitochondria. Importantly, the (photo)cytotoxicity of the complex further increased when the cells were pretreated with **BCN-Phos-5** or **BCN-Phos-6**. Our findings demonstrate that the theranostic potential of transition metal nitrone complexes can be enhanced through the strategic structural manipulation of their bioorthogonal reaction partners. We believe that our work will contribute to the development of effective mitochondria-targeting agents for diagnostic and therapeutic applications.

Author contributions

E. R. H. W., L. C.-C. L., P. K.-K. L., K. K.-W. L. and N. J. L. designed the project. E. R. H. W. carried out the synthesis and characterisation of the phosphonium cations. L. C.-C. L. carried out the synthesis and characterisation of the

iridium(III) nitrone complex and the cellular studies. P. K.-K. L. carried out the photophysical measurements and cellular studies. E. R. H. W., L. C.-C. L., P. K.-K. L., K. K.-W. L. and N. J. L. analysed the data and wrote the manuscript.

Conflicts of interest

There are no conflicts to declare.

Data availability

We confirm that all the relevant research data is contained with the manuscript and ESI.† No databases have been used and no references to such databases are contained in the manuscript or ESI.†

Acknowledgements

References

1 E. M. Sletten and C. R. Bertozzi, Bioorthogonal chemistry: fishing for selectivity in a sea of functionality, *Angew. Chem., Int. Ed.*, 2009, **48**, 6974.

2 S. L. Scinto, D. A. Bilodeau, R. Hincapie, W. Lee, S. S. Nguyen, M. Xu, C. W. am Ende, M. G. Finn, K. Lang, Q. Lin, J. P. Pezacki, J. A. Prescher, M. S. Robillard and J. M. Fox, Bioorthogonal chemistry, *Nat. Rev. Methods Primers*, 2021, **1**, 30.

3 J. C. Jewett and C. R. Bertozzi, Cu-free click cycloaddition reactions in chemical biology, *Chem. Soc. Rev.*, 2010, **39**, 1272.

4 B. L. Oliveira, Z. Guo and G. J. L. Bernardes, Inverse electron demand Diels–Alder reactions in chemical biology, *Chem. Soc. Rev.*, 2017, **46**, 4895.

5 T. K. Heiss, R. S. Dorn and J. A. Prescher, Bioorthogonal reactions of triarylphosphines and related analogues, *Chem. Rev.*, 2021, **121**, 6802.

6 X. Ji, Z. Pan, B. Yu, L. K. De La Cruz, Y. Zheng, B. Ke and B. Wang, Click and release: bioorthogonal approaches to "on-demand" activation of prodrugs, *Chem. Soc. Rev.*, 2019, **48**, 1077.

7 D. Wu, K. Yang, Z. Zhang, Y. Feng, L. Rao, X. Chen and G. Yu, Metal-free bioorthogonal click chemistry in cancer theranostics, *Chem. Soc. Rev.*, 2022, **51**, 1336.

8 Q. Fu, S. Shen, P. Sun, Z. Gu, Y. Bai, X. Wang and Z. Liu, Bioorthogonal chemistry for prodrug activation *in vivo*, *Chem. Soc. Rev.*, 2023, **52**, 7737.

9 V. Rigolot, C. Biot and C. Lion, To view your biomolecule, click inside the cell, *Angew. Chem., Int. Ed.*, 2021, **60**, 23084.

10 P. Shieh and C. R. Bertozzi, Design strategies for bioorthogonal smart probes, *Org. Biomol. Chem.*, 2014, **12**, 9307.

11 Y. Fu, X. Zhang, L. Wu, M. Wu, T. D. James and R. Zhang, Bioorthogonally activated probes for precise fluorescence imaging, *Chem. Soc. Rev.*, 2025, **54**, 201.

12 A. Yu, X. He, T. Shen, X. Yu, W. Mao, W. Chi, X. Liu and H. Wu, *Chem. Soc. Rev.*, 2025, **54**, 2984, DOI: **10.1039/D3CS00520H**.

13 L. K. B. Tam and D. K. P. Ng, "Click" for precise photodynamic therapy, *Mater. Chem. Front.*, 2023, **7**, 3184.

14 E. Kozma, M. Bojtár and P. Kele, Bioorthogonally assisted phototherapy: recent advances and prospects, *Angew. Chem., Int. Ed.*, 2023, **62**, e202303198.

15 Y. Chen, R. Guan, C. Zhang, J. Huang, L. Ji and H. Chao, Two-photon luminescent metal complexes for bioimaging and cancer phototherapy, *Coord. Chem. Rev.*, 2016, **310**, 16.

16 J. Li and T. Chen, Transition metal complexes as photosensitizers for integrated cancer theranostic applications, *Coord. Chem. Rev.*, 2020, **418**, 213355.

17 C.-P. Tan, Y.-M. Zhong, L.-N. Ji and Z.-W. Mao, Phosphorescent metal complexes as theranostic anticancer agents: combining imaging and therapy in a single molecule, *Chem. Sci.*, 2021, **12**, 2357.

18 L. C.-C. Lee and K. K.-W. Lo, Luminescent and photofunctional transition metal complexes: from molecular design to diagnostic and therapeutic applications, *J. Am. Chem. Soc.*, 2022, **144**, 14420.

19 L. C.-C. Lee and K. K.-W. Lo, Leveraging the photofunctions of transition metal complexes for the design of innovative phototherapeutics, *Small Methods*, 2024, **8**, 2400563.

20 K. K.-W. Lo, Molecular design of bioorthogonal probes and imaging reagents derived from photofunctional transition metal complexes, *Acc. Chem. Res.*, 2020, **53**, 32.

21 D. A. Bilodeau, K. D. Margison, M. Serhan and J. P. Pezacki, Bioorthogonal reactions utilizing nitrones as versatile dipoles in cycloaddition reactions, *Chem. Rev.*, 2021, **121**, 6699.

22 L. C.-C. Lee, J. C.-W. Lau, H.-W. Liu and K. K.-W. Lo, Conferring phosphorogenic properties on iridium(III)-based bioorthogonal probes through modification with a nitrone unit, *Angew. Chem., Int. Ed.*, 2016, **55**, 1046.

23 T. S.-M. Tang, H.-W. Liu and K. K.-W. Lo, Structural manipulation of ruthenium(II) polypyridine nitrone complexes to generate phosphorogenic bioorthogonal reagents for selective cellular labeling, *Chem. – Eur. J.*, 2016, **22**, 9649.

24 P. K.-K. Leung and K. K.-W. Lo, Modulation of emission and singlet oxygen photosensitisation in live cells utilising bioorthogonal phosphorogenic probes and protein tag technology, *Chem. Commun.*, 2020, **56**, 6074.

25 E. C.-L. Mak, Z. Chen, L. C.-C. Lee, P. K.-K. Leung, A. M.-H. Yip, J. Shum, S.-M. Yiu, V. W.-W. Yam and K. K.-W. Lo, Exploiting the potential of iridium(III) *bis*-nitrone complexes as phosphorogenic bifunctional reagents for phototheranostics, *J. Am. Chem. Soc.*, 2024, **146**, 25589.

6490 | *Inorg. Chem. Front.*, 2025, **12**, 6484–6493

This journal is © the Partner Organisations 2025

26 J. B. Spinelli and M. C. Haigis, The multifaceted contributions of mitochondria to cellular metabolism, *Nat. Cell Biol.*, 2018, **20**, 745.

27 R. Rizzuto, D. De Stefani, A. Raffaello and C. Mammucari, Mitochondria as sensors and regulators of calcium signalling, *Nat. Rev. Mol. Cell Biol.*, 2012, **13**, 566.

28 D. R. Green and J. C. Reed, Mitochondria and apoptosis, *Science*, 1998, **281**, 1309.

29 S. Vyas, E. Zaganjor and M. C. Haigis, Mitochondria and cancer, *Cell*, 2016, **166**, 555.

30 M. T. Lin and M. F. Beal, Mitochondrial dysfunction and oxidative stress in neurodegenerative diseases, *Nature*, 2006, **443**, 787.

31 S. Fulda, L. Galluzzi and G. Kroemer, Targeting mitochondria for cancer therapy, *Nat. Rev. Drug Discovery*, 2010, **9**, 447.

32 L. B. Chen, Mitochondrial membrane potential in living cells, *Annu. Rev. Cell Biol.*, 1988, **4**, 155.

33 J. Zielonka, J. Joseph, A. Sikora, M. Hardy, O. Ouari, J. Vasquez-Vivar, G. Cheng, M. Lopez and B. Kalyanaraman, Mitochondria-targeted triphenylphosphonium-based compounds: syntheses, mechanisms of action, and therapeutic and diagnostic applications, *Chem. Rev.*, 2017, **117**, 10043.

34 S. H. Alamudi, R. Satapathy, J. Kim, D. Su, H. Ren, R. Das, L. Hu, E. Alvarado-Martínez, J. Y. Lee, C. Hoppmann, E. Peña-Cabrera, H.-H. Ha, H.-S. Park, L. Wang and Y.-T. Chang, Development of background-free tame fluorescent probes for intracellular live cell imaging, *Nat. Commun.*, 2016, 7, 11964.

35 A. Vázquez, R. Dzijak, M. Dračínský, R. Rampmaier, S. J. Siegl and M. Vrabel, Mechanism-based fluorogenic *trans*-cyclooctene–tetrazine cycloaddition, *Angew. Chem., Int. Ed.*, 2017, **56**, 1334.

36 Y. Lee, W. Cho, J. Sung, E. Kim and S. B. Park, Monochromophoric design strategy for tetrazine-based colorful bioorthogonal probes with a single fluorescent core skeleton, *J. Am. Chem. Soc.*, 2018, **140**, 974.

37 S. H. Alamudi, D. Su, K. J. Lee, J. Y. Lee, J. L. Belmonte-Vázquez, H.-S. Park, E. Peña-Cabrera and Y.-T. Chang, A palette of background-free tame fluorescent probes for intracellular multi-color labelling in live cells, *Chem. Sci.*, 2018, **9**, 2376.

38 P. Werther, K. Yserentant, F. Braun, N. Kaltwasser, C. Popp, M. Baalmann, D.-P. Herten and R. Wombacher, Live-cell localization microscopy with a fluorogenic and self-blinking tetrazine probe, *Angew. Chem., Int. Ed.*, 2020, **59**, 804.

39 M. Bojtár, K. Németh, F. Domahidy, G. Knorr, A. Verkman, M. Kállay and P. Kele, Conditionally activatable visible-light photocages, *J. Am. Chem. Soc.*, 2020, **142**, 15164.

40 W. Mao, J. Tang, L. Dai, X. He, J. Li, L. Cai, P. Liao, R. Jiang, J. Zhou and H. Wu, A general strategy to design highly fluorogenic far-red and near-infrared tetrazine bioorthogonal probes, *Angew. Chem., Int. Ed.*, 2021, **60**, 2393.

41 W. Mao, W. Chi, X. He, C. Wang, X. Wang, H. Yang, X. Liu and H. Wu, Overcoming spectral dependence: a general strategy for developing far-red and near-infrared ultrafluorogenic tetrazine bioorthogonal probes, *Angew. Chem., Int. Ed.*, 2022, **61**, e202117386.

42 D. Kim, H. Son and S. B. Park, Ultrafluorogenic monochromophore-type BODIPY-tetrazine series for dual-color bioorthogonal imaging with a single probe, *Angew. Chem., Int. Ed.*, 2023, **62**, e202310665.

43 S. Segawa, J. Wu, R. T. K. Kwok, T. T. W. Wong, X. He and B. Z. Tang, Co-aggregation as a simple strategy for preparing fluorogenic tetrazine probes with on-demand fluorogen selection, *Angew. Chem., Int. Ed.*, 2024, **63**, e202313930.

44 Y. Deng, T. Shen, X. Yu, J. Li, P. Zou, Q. Gong, Y. Zheng, H. Sun, X. Liu and H. Wu, Tetrazine-isonitrile bioorthogonal fluorogenic reactions enable multiplex labeling and wash-free bioimaging of live cells, *Angew. Chem., Int. Ed.*, 2024, **63**, e202319853.

45 S. Segawa, X. Ou, T. Shen, T. Ryu, Y. Ishii, H. H. Y. Sung, I. D. Williams, R. T. K. Kwok, K. Onda, K. Miyata, X. He, X. Liu and B. Z. Tang, Matthew effect: general design strategy of ultra-fluorogenic nanoprobes with amplified dark–bright states in aggregates, *Aggregate*, 2024, **5**, e499.

46 H. Son, D. Kim, S. Kim, W. G. Byun and S. B. Park, Unveiling the structure-fluorogenic property relationship of Seoul-Fluor-derived bioorthogonal tetrazine probes, *Angew. Chem., Int. Ed.*, 2025, **64**, e202421982.

47 Z. Xue, R. Zhu, S. Wang, J. Li, J. Han, J. Liu and S. Han, Organelle-directed Staudinger reaction enabling fluorescence-on resolution of mitochondrial electropotentials via a self-immolative charge reversal probe, *Anal. Chem.*, 2018, **90**, 2954.

48 Y. Shi, X. Zou, S. Wen, L. Gao, J. Li, J. Han and S. Han, An organelle-directed chemical ligation approach enables dual-color detection of mitophagy, *Autophagy*, 2021, **17**, 3475.

49 Y. Zheng, X. Ji, B. Yu, K. Ji, D. Gallo, E. Csizmadia, M. Zhu, M. R. Choudhury, L. K. C. De La Cruz, V. Chittavong, Z. Pan, Z. Yuan, L. E. Otterbein and B. Wang, Enrichment-triggered prodrug activation demonstrated through mitochondria-targeted delivery of doxorubicin and carbon monoxide, *Nat. Chem.*, 2018, **10**, 787.

50 R. Dzijak, J. Galeta, A. Vázquez, J. Kozák, M. Matoušová, H. Fulka, M. Dračínský and M. Vrabel, Structurally redesigned bioorthogonal reagents for mitochondria-specific prodrug activation, *JACS Au*, 2021, **1**, 23.

51 M. Liu, Z. Liu, G. Qin, J. Ren and X. Qu, Bioorthogonally activatable autophagy-tethering compounds for aptamer-guided mitochondrial degradation, *Nano Lett.*, 2023, **23**, 4965.

52 J. Kim, Y. Xu, J. H. Lim, J. Y. Lee, M. Li, J. M. Fox, M. Vendrell and J. S. Kim, Bioorthogonal activation of deep red photoredox catalysis inducing pyroptosis, *J. Am. Chem. Soc.*, 2025, **147**, 701.

53 B.-L. Li, S. Li, C. Zhang, Y. Zhou, X. Zhao and Z. Yu, Photoclick and release for spatiotemporally localized thera-

This journal is © the Partner Organisations 2025

Inorg. Chem. Front., 2025, **12**, 6484–6493 | **6491**

nostics of single cells via *in situ* generation of 1,3-diaryl-1*H*-benzo[*f*]indazole-4,9-dione, *Angew. Chem., Int. Ed.*, 2025, **64**, e202416111.

54 Y. Chen, R. Zhao, C. Tang, C. Zhang, W. Xu, L. Wu, Y. Wang, D. Ye and Y. Liang, Design and development of a bioorthogonal, visualizable and mitochondria-targeted hydrogen sulfide (H₂S) delivery system, *Angew. Chem., Int. Ed.*, 2022, **61**, e202112734.

55 L. Huang, P. K.-K. Leung, L. C.-C. Lee, G.-X. Xu, Y.-W. Lam and K. K.-W. Lo, Photofunctional cyclometallated iridium (III) polypyridine methylsulfone complexes as sulfhydryl-specific reagents for bioconjugation, bioimaging and photocytotoxic applications, *Chem. Commun.*, 2022, **58**, 10162.

56 T. I. Rokitskaya, E. A. Kotova, V. B. Luzhkov, R. S. Kirsanov, E. V. Aleksandrova, G. A. Korshunova, V. N. Tashlitsky and Y. N. Antonenko, Lipophilic ion aromaticity is not important for permeability across lipid membranes, *Biochim. Biophys. Acta, Biomembr.*, 2021, **1863**, 183483.

57 E. R. H. Walter, L. C.-C. Lee, P. K.-K. Leung, K. K.-W. Lo and N. J. Long, Mitochondria-targeting biocompatible fluorescent BODIPY probes, *Chem. Sci.*, 2024, **15**, 4846.

58 E. R. H. Walter, P. K.-K. Leung, L. C.-C. Lee, K. K.-W. Lo and N. J. Long, Potent BODIPY-based photosensitisers for selective mitochondrial dysfunction and effective photodynamic therapy, *J. Mater. Chem. B*, 2024, **12**, 10409.

59 Z. Hu, Y. Sim, O. L. Kon, W. H. Ng, A. J. M. Ribeiro, M. J. Ramos, P. A. Fernandes, R. Ganguly, B. Xing, F. García and E. K. L. Yeow, Unique triphenylphosphonium derivatives for enhanced mitochondrial uptake and photodynamic therapy, *Bioconjugate Chem.*, 2017, **28**, 590.

60 A. J. Smith, P. J. Gawne, M. T. Ma, P. J. Blower, R. Southworth and N. J. Long, Synthesis, gallium-68 radiolabelling and biological evaluation of a series of triarylphosphonium-functionalized DO3A chelators, *Dalton Trans.*, 2018, **47**, 15448.

61 A. J. Smith, B. E. Osborne, G. P. Keeling, P. J. Blower, R. Southworth and N. J. Long, DO2A-based ligands for gallium-68 chelation: synthesis, radiochemistry and *ex vivo* cardiac uptake, *Dalton Trans.*, 2020, **49**, 1097.

62 B. E. Osborne, T. T. C. Yue, E. C. T. Waters, F. Baark, R. Southworth and N. J. Long, Synthesis and *ex vivo* biological evaluation of gallium-68 labelled NODAGA chelates assessing cardiac uptake and retention, *Dalton Trans.*, 2021, **50**, 14695.

63 A. Haslop, L. Wells, A. Gee, C. Plisson and N. Long, One-pot multi-tracer synthesis of novel ¹⁸F-labeled PET imaging agents, *Mol. Pharmaceutics*, 2014, **11**, 3818.

64 M. Jiang, J. Wu, W. Liu, H. Ren, W. Zhang, C.-S. Lee and P. Wang, Self-assembly of amphiphilic porphyrins to construct nanoparticles for highly efficient photodynamic therapy, *Chem. – Eur. J.*, 2021, **27**, 11195.

65 Q. Zeng, Q. Guo, Y. Yuan, Y. Yang, B. Zhang, L. Ren, X. Zhang, Q. Luo, M. Liu, L.-S. Bouchard and X. Zhou, Mitochondria targeted and intracellular biothiol triggered

hyperpolarized ¹²⁹Xe magnetofluorescent biosensor, *Anal. Chem.*, 2017, **89**, 2288.

66 K. Suzuki, A. Kobayashi, S. Kaneko, K. Takehira, T. Yoshihara, H. Ishida, Y. Shiina, S. Oishi and S. Tobita, Reevaluation of absolute luminescence quantum yields of standard solutions using a spectrometer with an integrating sphere and a back-thinned CCD detector, *Phys. Chem. Chem. Phys.*, 2009, **11**, 9850.

67 A. A. Abdel-Shafi, P. D. Beer, R. J. Mortimer and F. Wilkinson, Photosensitized generation of singlet oxygen from vinyl linked benzo-crown-ether–bipyridyl ruthenium (II) complexes, *J. Phys. Chem. A*, 2000, **104**, 192.

68 K. K.-W. Lo, J. S.-W. Chan, L.-H. Lui and C.-K. Chung, Novel luminescent cyclometalated iridium(III) diimine complexes that contain a biotin moiety, *Organometallics*, 2004, **23**, 3108.

69 K. K.-W. Lo, C.-K. Chung and N. Zhu, Nucleic acid intercalators and avidin probes derived from luminescent cyclometalated iridium(III)–dipyridoquinoxaline and –dipyridophenazine complexes, *Chem. – Eur. J.*, 2006, **12**, 1500.

70 K. K.-W. Lo, K. Y. Zhang, C.-K. Chung and K. Y. Kwok, Synthesis, photophysical and electrochemical properties, and protein-binding studies of luminescent cyclometalated iridium(III) bipyridine estradiol conjugates, *Chem. – Eur. J.*, 2007, **13**, 7110.

71 K. K.-W. Lo, K. Y. Zhang, S.-K. Leung and M.-C. Tang, Exploitation of the dual-emissive properties of cyclometalated iridium(III)–polypyridine complexes in the development of luminescent biological probes, *Angew. Chem., Int. Ed.*, 2008, **47**, 2213.

72 J. S.-Y. Lau, P.-K. Lee, K. H.-K. Tsang, C. H.-C. Ng, Y.-W. Lam, S.-H. Cheng and K. K.-W. Lo, Luminescent cyclometalated iridium(III) polypyridine indole complexes–synthesis, photophysics, electrochemistry, protein-binding properties, cytotoxicity, and cellular uptake, *Inorg. Chem.*, 2009, **48**, 708.

73 L. C.-C. Lee, H. M.-H. Cheung, H.-W. Liu and K. K.-W. Lo, Exploitation of environment-sensitive luminophores in the design of sydnone-based bioorthogonal imaging reagents, *Chem. – Eur. J.*, 2018, **24**, 14064.

74 Q. Zhang, R. Cao, H. Fei and M. Zhou, Mitochondria-targeting phosphorescent iridium(III) complexes for living cell imaging, *Dalton Trans.*, 2014, **43**, 16872.

75 J. Liu, Y. Chen, G. Li, P. Zhang, C. Jin, L. Zeng, L. Ji and H. Chao, Ruthenium(II) polypyridyl complexes as mitochondria-targeted two-photon photodynamic anticancer agents, *Biomaterials*, 2015, **56**, 140.

76 W. Lv, Z. Zhang, K. Y. Zhang, H. Yang, S. Liu, A. Xu, S. Guo, Q. Zhao and W. Huang, A mitochondria-targeted photosensitizer showing improved photodynamic therapy effects under hypoxia, *Angew. Chem., Int. Ed.*, 2016, **55**, 9947.

77 H. Yuan, Z. Han, Y. Chen, F. Qi, H. Fang, Z. Guo, S. Zhang and W. He, Ferroptosis photoinduced by new cyclometalated iridium(III) complexes and its synergism with apoptosis in tumor cell inhibition, *Angew. Chem., Int. Ed.*, 2021, **60**, 8174.

6492 | *Inorg. Chem. Front.*, 2025, **12**, 6484–6493

This journal is © the Partner Organisations 2025

78 W. Xu, H. Wang, Y. Guang, Z. Pan, K. Chen, T. Ma and J. Zhang, A mitochondria-targeted iridium(III) phosphorescent probe for selective detection of hypochlorite in living cells, *Chem. – Asian J.*, 2025, **20**, e202401351.

79 H. Fu, S. Wang, Y. Gong, H. Dong, K. Lai, Z. Yang, C. Fan, Z. Liu and L. Guo, Triphenylphosphine-modified cyclometalated iridium[III] complexes as mitochondria-targeting anticancer agents with enhanced selectivity, *Bioorg. Chem.*, 2025, **155**, 108148.

80 S. Li, H. Yuan, X.-Z. Yang, X. Xu, W. Yu, Y. Wu, S. Yao, J. Xie, W. He, Z. Guo and Y. Chen, Synergistic antitumor immunotherapy via mitochondria regulation in macrophages and tumor cells by an iridium photosensitizer, *ACS Cent. Sci.*, 2025, **11**, 441.

This journal is © the Partner Organisations 2025

Inorg. Chem. Front., 2025, **12**, 6484–6493 | **6493**